

Sub-Poissonian multiplicity distributions in jets produced in hadron collisions

Han Wei Ang,^{1,*} Maciej Rybczyński,^{2,†} Grzegorz Wilk,^{3,‡} and Zbigniew Włodarczyk^{2,§}

¹*Department of Physics, National University of Singapore, Singapore 117551*

²*Institute of Physics, Jan Kochanowski University, 25-406 Kielce, Poland*

³*National Centre for Nuclear Research, Warsaw 00-681, Poland*

In this work we show that the proper analysis and interpretation of the experimental data on the multiplicity distributions of charged particles produced in jets measured in the ATLAS experiment at the LHC indicates their sub-Poissonian nature. We also show how, by using the recurrent relations and combinants of these distributions, one can obtain new information contained in them and otherwise unavailable, which may broaden our knowledge of the particle production mechanism.

PACS numbers: 13.85.Hd, 25.75.Gz, 02.50.Ey

I. INTRODUCTION

The experimentally measured multiplicity distributions $P(N)$ of the produced particles are the main source of information about the dynamics of their production processes [1, 2]. In the theoretical description they are characterized by the generating functions,

$$G(z) = \sum_{N=0}^{\infty} P(N)z^N, \quad (1)$$

such that

$$P(N) = \frac{1}{N!} \left. \frac{d^N G(z)}{dz^N} \right|_{z=0}. \quad (2)$$

Preliminary information about $P(N)$ is provided by the moments of this distribution,

$$m_k = \sum_{N=0}^{\infty} (N-c)^k P(N). \quad (3)$$

In many cases, it is sufficient to analyze only the two lowest moments, namely the mean value $\langle N \rangle = m_1$ being the first raw moment ($c = 0$), and variance $Var(N) = m_2$, being the second central moment ($c = \langle N \rangle$).

Another way to characterize $P(N)$ is through a recursive formula,

$$(N+1)P(N+1) = g(N)P(N), \quad (4)$$

that connects adjacent values of $P(N)$ for the production of N and $(N+1)$ particles. It is assumed here that every $P(N)$ is determined only by the next lower $P(N-1)$ value. In other words, a relationship with others $P(N-j)$ for $j > 1$ is indirect. The final algebraic form of $P(N)$ is determined by the function $g(N)$. In its simplest form,

$g(N)$ is assumed to be a linear function of N given by $g(N) = \alpha + \beta N$. This form is enough to define commonly known and widely used distributions like Poisson Distribution (PD), for which $\beta = 0$, Binomial Distribution (BD) (for which $\beta < 0$) or Negative Binomial Distribution (for which $\beta > 0$). In general, by selecting the appropriate model, the form $g(N)$ can be chosen in such a way that the corresponding $P(N)$ describes the experimental data (for example, by introducing higher order terms [3] or by using its more involved forms [4, 5]).

The more promising approach is to use $g(N)$ which contains information about the interrelationship between the multiplicity N and all smaller multiplicities recursively,

$$(N+1)P(N+1) = \langle N \rangle \sum_{j=0}^N C_j P(N-j). \quad (5)$$

The memory of that relationship is encoded in coefficients C_j called *modified combinants*. They were introduced and intensively discussed in [6–13]. By inverting the recursion (5) we obtain an equation that allows us to determine C_j from the measured $P(N)$,

$$\langle N \rangle C_j = (j+1) \left[\frac{P(j+1)}{P(0)} \right] - \langle N \rangle \sum_{i=0}^{j-1} C_i \left[\frac{P(j-i)}{P(0)} \right] \quad (6)$$

(provided we have sufficient statistics). Modified combinants are closely related to *combinants* C_j^* ,

$$C_j = \frac{j+1}{\langle N \rangle} C_{j+1}^*, \quad (7)$$

introduced in [14–16] by means of the generating functions $G(z)$ as

$$\langle N \rangle C_j^* = \frac{1}{j!} \left. \frac{d^{j+1} \ln G(z)}{dz^{j+1}} \right|_{z=0}, \quad (8)$$

which have been discussed and used in many publications [1, 2, 17–21].

Modified combinants are complementary to the commonly used factorial moments, F_q and cumulant factorial

* ang.h.w@u.nus.edu

† maciej.rybczynski@ujk.edu.pl

‡ grzegorz.wilk@ncbj.gov.pl

§ zbigniew.wlodarczyk@ujk.edu.pl

moments, K_q (see Appendix A for details). They differ in that while C_j 's depend only on multiplicities smaller than their rank, K_q 's require the knowledge of all $P(N)$'s and are therefore very sensitive to possible limitations of the available phase space [1, 2]. However, both C_j and K_q share the property of additivity. It turns out that most of the measured multiplicity distributions $P(N)$ give oscillatory combinants C_j with increasing index j which arise due to the presence of a BD component in the measured $P(N)$ [7–12].

Combinants are believed to be best suited for the study of sparsely populated areas of phase space (while cumulants are better suited for the study of densely populated areas) [1, 2]. This feature makes them a potentially important tool for studying $P(N)$ in jets where the number of produced particles is small (on the order of ~ 10). However, the ATLAS data [22] do not include $P(0)$, which is crucial for their determination. This means that in our analysis, we must extrapolate the recurrent relation in Eq. (4) to evaluate $P(0)$ and use the combinants only for additional verification of our conclusions.

In the next Section we provide details concerning ATLAS data with particular attention to the fact that the measured multiplicity distributions in the jets are clearly sub-Poissonian in character (with details depending on the phase-space covered). This observation will be our main point for further discussion and calculations described in Sections III and IV. Section V summarizes and concludes our work.

II. MULTIPLICITY DISTRIBUTIONS OF PARTICLES IN ATLAS JETS

ATLAS data [22] of jets measured in proton-proton collisions at an energy $\sqrt{s} = 7$ TeV (using a minimum bias trigger) were taken (data used here come from [23]). Jets were reconstructed using the anti- k_t algorithm applied to charged particles produced in very narrow cones defined by radius parameter $R = \sqrt{\Delta\eta^2 + \Delta\phi^2}$ (where $\Delta\phi$ and $\Delta\eta$ are the azimuthal angle and the pseudorapidity of the hadrons relative to that of the jet respectively. Here, $\eta = -\ln \tan \theta$, with θ being the polar angle), with $R = 0.4$ and again at $R = 0.6$. Only data with high statistics within acceptable regions of phase space are selected. They are obtained over 5 different transverse momentum ranges across 4 rapidity ranges, giving a total of 20 possible combinations for each of the two radius parameters (with radius parameters $R = 0.4$ and $R = 0.6$, respectively).

So far, the ATLAS data have been carefully analyzed in terms of possible self-similarity between p_T distribution of jets and p_T distributions of particles in these jets [24]. Indeed, their detailed analysis clearly indicates the self-similarity of the particle distributions in jets and the distributions of the jets themselves, indicative of the existence of a common mechanism behind all these processes.

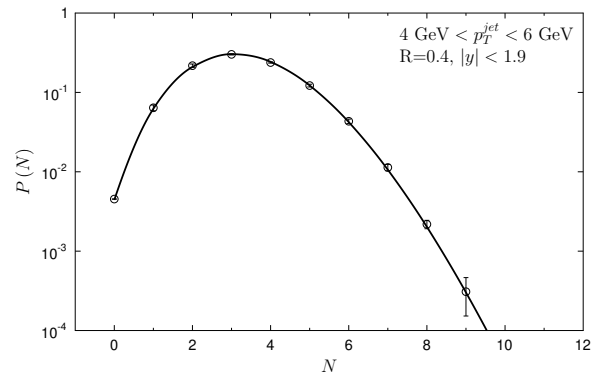


FIG. 1. Multiplicity distribution of charged particles per jet with $4 \text{ GeV} < p_T^{\text{jet}} < 6 \text{ GeV}$, over the full measured rapidity range $|y| < 1.9$, with radius parameter $R = 0.4$. Points show data from ATLAS experiment [22]. $P(N = 0)$ comes from extrapolation of experimental recurrent relation $g(N)$ to $N = 0$. The curve fitting this data comes from Eq. (13) with parameters $\alpha = 14.1$ and $\delta = 1.07$.

Taking advantage of the fact that ATLAS also publishes data for multiplicity distributions of particles produced in observed jets, we extend this analysis to study the nature of these distributions. The first observation is that the multiplicity distributions of the particles in the jets observed in the ATLAS experiment are sub-Poissonian, cf. Fig. 1 where $\text{Var}(N) < \langle N \rangle$. Though BD is a possible sub-Poissonian distribution for $g(N)$, the plot in Fig. 2 derived from the recursive relationship in Eq. (4) is non-linear.

It means therefore that one should switch to scenario inspired by the possible non-linear form of recursion $g(N)$ such as

$$g(N) = (N + 1) \frac{P(N + 1)}{P(N)} = \frac{\alpha}{(N + 1)^\delta}. \quad (9)$$

As shown in Fig. 2, such form with $\delta = 1.07$ fits data

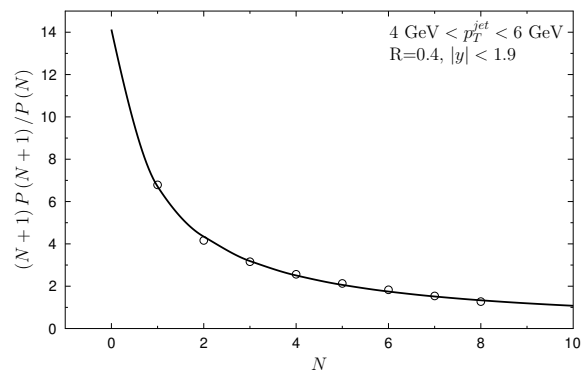


FIG. 2. Recurrent relations. Points show $g(N)$ for experimental $P(N)$ from Fig. 1. Curve fit using $g(N)$ from Eq. (9) with $\alpha = 14.1$ and $\delta = 1.07$.

very well. Therefore, we note that for

$$(N+1) \frac{P(N+1)}{P(N)} = \alpha \quad (10)$$

we have the PD with,

$$P(N) = c \frac{\alpha^N}{N!} \quad \text{where} \quad \alpha = \langle N \rangle, \quad c = \exp(-\alpha). \quad (11)$$

If we change this recursive relationship to a nonlinear one given by

$$(N+1)^{1+\delta} \frac{P(N+1)}{P(N)} = \alpha, \quad (12)$$

we get sub-Poissonian distribution,

$$P(N) = c \frac{\alpha^N}{(N!)^{1+\delta}}, \quad (13)$$

where $c = P(0)$ is a normalization factor. In Fig. 1 we present a comparison of this multiplicity distribution with the experimental data from ATLAS.

Once we know $P(0)$ from extrapolation of experimental recurrent relation $g(N)$ to $N = 0$, we are able to determine the corresponding modified combinants from the measured multiplicity distributions $P(N)$ using Eq. (6) (which is important because in ATLAS, the $P(0)$ data points are not directly measured). The C_j 's derived in this way are plotted in Fig. 3 as red circles. They can now be compared with the combinants obtained in the same way but from the theoretical sub-Poissonian distribution $P(N)$ given by Eq. (13). The corresponding results are plotted in Fig. 3 as black squares. We observe characteristic oscillatory behaviour of modified combinants with only rough amplitude agreement. Despite nice agreement of multiplicity distributions, shown in Fig. 1, the mentioned combinants indicate difference between fit and experimental data.

In the event where $\delta = 1$ Eq. (13) can be written in a closed form given by,

$$P(N) = \frac{1}{I_0(2\sqrt{\alpha})} \frac{\alpha^N}{(N!)^2}, \quad (14)$$

where

$$\alpha = \langle N^2 \rangle \quad \text{and} \quad c = P(0) = \frac{1}{I_0(2\sqrt{\alpha})}, \quad (15)$$

with I_0 being the Bessel function of the first kind. In this case ($\delta = 1$) the theoretical C_j 's are given by the recurrent relation,

$$\langle N \rangle C_j = \frac{(j+1)\alpha^{j+1}}{[(j+1)!]^2} - \langle N \rangle \sum_{i=0}^{j-1} C_i \frac{\alpha^{j-i}}{[(j-i)!]^2}, \quad (16)$$

and are of the form

$$\langle N \rangle C_j = (-1)^j \beta_j \alpha^{j+1} \quad (17)$$

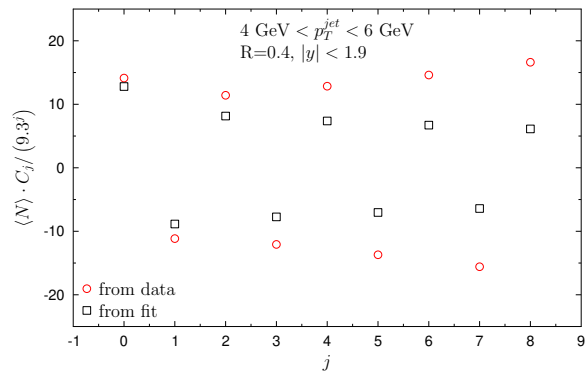


FIG. 3. Comparison of C_j for multiplicity distributions from Fig. 1. Red circles: C_j from data on $P(N)$ from Fig. 1. Black squares: from theoretical $P(N)$ defined by Eq.(13).

where the numbers β_j are rational: $\beta_0 = 1$, $\beta_1 = \frac{1}{2}$, $\beta_2 = \frac{1}{3}$, $\beta_3 = \frac{11}{48}$, $\beta_4 = \frac{19}{120}$, $\beta_5 = \frac{473}{4320}, \dots$. They were first calculated by Euler in relation to the positive zeros γ_l of the Bessel function $J_0(z)$ as [25]

$$\beta_{j+1} = \sum_{l=1}^{\infty} \left(\frac{2}{\gamma_l} \right)^{2(j+l)}, \quad j = 0, 1, 2, \dots \quad (18)$$

For $j \geq 1$ coefficients β_j can be approximated by

$$\beta_j \cong \exp \left[-\frac{j+1}{e} \right]. \quad (19)$$

At this point, it is worth noting that C_j can help in the search for the correct $P(N)$. Based on our experience thus far, let us assume, that strongly oscillating C_j (especially with period, as seen in Fig. 3) indicate the presence of a single-component BD in some form. On

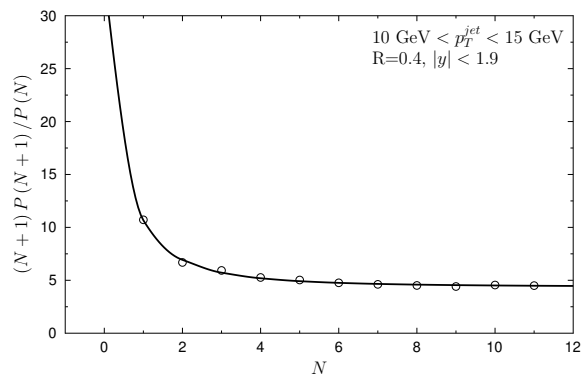


FIG. 4. Recurrent relations $g(N)$ for multiplicity distributions $P(N)$ over the full measured rapidity range $|y| < 1.9$, in jets with radius parameter $R = 0.4$ and transverse momentum range $10 \text{ GeV} < p_T^{\text{jet}} < 15 \text{ GeV}$. Points: $g(N)$ from experimental data [22]. Curve: fit using $g(N)$ from Eq. (20) with parameters: $\alpha = 29.4$, $\delta = 2.20$ and $\alpha_0 = 4.37$.

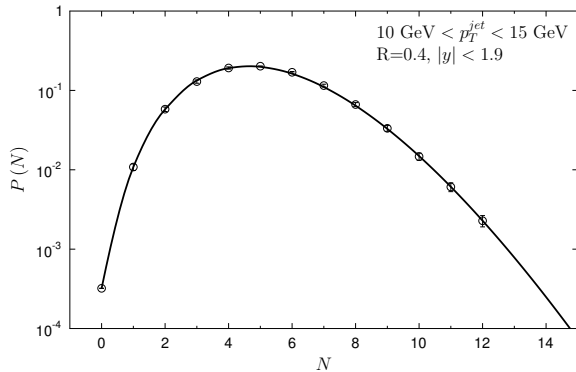


FIG. 5. Points: $P(N)$ from ATLAS data for jets with $10 \text{ GeV} < p_T^{\text{jet}} < 15 \text{ GeV}$ and radius parameter $R = 0.4$, over the full measured rapidity range $|y| < 1.9$. The curve fitting these data comes from Eq.(21) with parameters: $c = 3.2 \cdot 10^{-4}$, $\alpha = 29.4$, $\alpha_0 = 4.37$ and $\delta = 2.20$.

closer inspection, it is clear that this cannot be the case since the amplitude of oscillations of C_j in Fig. 3 grows approximately as 9.3^j with j . Should these C_j originate from a single-component BD with amplitudes given by $[p/(1-p)]^j$, it would mean that $p > 0.8$. In addition, to reproduce $\langle N \rangle = Kp \sim 3.3$ as observed in data, one would require $K < 5$. Taken together, these would limit us to multiplicities of $N < 5$. This is in contradiction with the measured $P(N)$ where the observed multiplicities $N = 5$. By continuing to stick to BD, our previous experiences [7, 9–11] tell us that a potential solution might be to use the sum of two BD's instead of one. However, as we will show in the Appendix B, it is not possible to describe both $P(N)$ and its corresponding C_j with this approach.

Continuing the approach based on $g(N)$, it turns out that with the increase in p_T of jets (corresponding to an

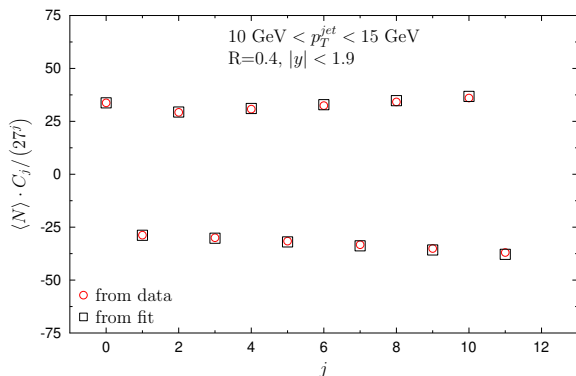


FIG. 6. Comparison of C_j for multiplicity distribution in jets. Red circles: C_j from data on $P(N)$, black squares: from theoretical $P(N)$ defined by Eq.(21). Parameters the same as in Fig. 5.

increase of $\langle N \rangle$ in our case), we observe a deviation from the form of $g(N)$ given in Eq. (9). The modified $g(N)$ can be made to describe data if expressed as a recursive relation given by (see Fig. 4)

$$g(N) = (N+1) \frac{P(N+1)}{P(N)} = \frac{\alpha}{(N+1)^\delta} + \alpha_0, \quad (20)$$

leading to the multiplicity distribution (see Fig. 5)

$$P(N) = \frac{c}{N!} \prod_{i=1}^N \left(\frac{\alpha}{i^\delta} + \alpha_0 \right) \quad (21)$$

with $c = P(0)$. The corresponding C_j are shown in Fig. 6.

Note that for integer parameter δ , Eq. (21) has closed analytical form, namely for $\delta = 1$

$$P(N) = P(0) \frac{\alpha_0^N}{(N!)^2} \frac{\Gamma\left(1 + \frac{\alpha}{\alpha_0} + N\right)}{\Gamma\left(1 + \frac{\alpha}{\alpha_0}\right)}, \quad (22)$$

while for $\delta = 2$

$$P(N) = P(0) \frac{\alpha_0^N}{(N!)^3} \cdot \frac{\Gamma\left(1 - \sqrt{\frac{-\alpha}{\alpha_0}} + N\right) \Gamma\left(1 + \sqrt{\frac{-\alpha}{\alpha_0}} + N\right)}{\Gamma\left(1 - \sqrt{\frac{-\alpha}{\alpha_0}}\right) \Gamma\left(1 + \sqrt{\frac{-\alpha}{\alpha_0}}\right)}, \quad (23)$$

and for higher value of δ we have product of δ Pochhammer symbols,

$$(x_l)_N = \frac{\Gamma(x_l + N)}{\Gamma(x_l)}, \quad (24)$$

where $x_l = 1 + (-1)^l (-1)^{l/\delta} (\alpha/\alpha_0)^{1/\delta}$ for $l = 0, 1, \dots, \delta - 1$.

III. POSSIBLE EXPLANATION: MULTIPLICITY DEPENDENT BIRTH AND DEATH RATES

To interpret the results shown in the previous section, note that Eq. (13) actually represents the so-called COM-Poisson distribution introduced by Conway and Maxwell [26] as a model for steady state queuing systems with state-dependent arrival or service rates (in other words, birth-death process with Poisson arrival rate and exponential service rate). It was rediscovered in [27] where the term *Conway-Maxwell-Poisson* was proposed and a detailed study of its properties and applications was performed. More recent studies can be found in [28, 29]. To our best knowledge, this distribution has not been used in the analysis of multiplicity distributions of particles produced in multiparticle production processes.

We will now show that the form of the COM-Poissonian distribution can be obtained from a stochastic Markov process with multiplicity-dependent birth and death rates denoted by λ_N and μ_N , respectively [30]. Let $P(N, t)$ be the probability of having N particles at time t and let us consider a very general birth-death process given by the following equations:

$$P'(0, t) = -\lambda_0 P(0, t) + \mu_1 P(1, t), \quad (25)$$

$$P'(N, t) = -(\lambda_N + \mu_N) P(N, t) + \lambda_{N-1} P(N-1, t) + \mu_{N+1} P(N+1, t). \quad (26)$$

If we assume the forms

$$\lambda_N = \frac{\lambda}{(N+1)^a} \quad \text{and} \quad \mu_N = N^b \mu, \quad (27)$$

we get

$$-\left[\frac{\lambda}{(N+1)^a} + N^b \mu \right] P(N) + \frac{\lambda}{N^a} P(N-1) + (N+1)^b \mu P(N+1) = 0 \quad (28)$$

for the steady state, where $P'(N, t) = 0$. If we denote

$$\frac{\lambda}{\mu} = \alpha \quad (29)$$

we can re-write Eq. (28) as

$$-\frac{\alpha}{(N+1)^a} P(N) - N^b P(N) + \frac{\alpha}{N^a} P(N-1) + (N+1)^b P(N+1) = 0 \quad (30)$$

which leads to the recurrent relation

$$(N+1)^b P(N+1) = \frac{\alpha}{(N+1)^a} P(N). \quad (31)$$

Further simplifications can be made by writing

$$a + b = \nu \quad (32)$$

which gives us

$$\frac{P(N+1)}{P(N)} = \frac{\alpha}{(N+1)^\nu}. \quad (33)$$

For $\delta = \nu - 1$, this is just the recurrent form of COM-Poisson distribution defined by Eq. (12). The condition in Eq. (32) has allowed us to successfully re-parameterize the recurrent relation of Eq. (33) using α and $\nu = a + b$. This corresponds to the entire class of Markov processes previously characterized by parameters a and b with the birth and death rates given in Eq. (27).

However, to describe the distribution defined by equations (20) and (21) (which is no longer COM-Poisson distribution) still using the birth-death process we need to add an additional term λ^* to the birth rate λ_N in the form given by

$$\lambda_N = \frac{\lambda}{(N+1)^a} + \lambda^* (N+1)^{(b-1)}. \quad (34)$$

If we substitute (34) into (26) and denote

$$\frac{\lambda^*}{\mu} = \alpha_0 \quad (35)$$

we get the recurrent relation

$$\frac{P(N+1)}{P(N)} = \frac{\alpha}{(N+1)^\nu} + \frac{\alpha_0}{N+1} \quad (36)$$

corresponding to Eq. (20).

IV. SUMMARY OF RESULTS

The ATLAS data suitable for our purposes cover 5 different ranges of transverse momentum, each further divided into 4 different rapidity ranges totalling 20 different fragments of the phase space. In previous sections we have plotted examples of multiplicity distributions and their corresponding combinants. Figs. 1 and 3 show the plots for $4 \text{ GeV} < p_T^{jet} < 6 \text{ GeV}$ at $|y| < 1.9$ with $R = 0.4$ while Figs. 5 and 6 show that for $10 \text{ GeV} < p_T^{jet} < 15 \text{ GeV}$. Instead of showing all figures for $P(N)$ and C_j which we have calculated for each possible $g(N)$ given by Eq. (20) and $P(N)$ using Eq. (21), the presented values of the parameters in are described by the formula

$$\langle N \rangle |C_j| = AB^j. \quad (37)$$

With increasing values of transverse momenta of jets, p_T^{jet} , the mean multiplicity in jet grows and affects parameters given in the tables. In Table I the parameters depend on $\langle N \rangle$ in the following ways:

$$\delta = 0.94 + \left(\frac{\langle N \rangle}{4.9} \right)^{4.4}, \quad (38)$$

$$\alpha_0 = -4.94 + 1.7 \langle N \rangle, \quad (39)$$

$$\alpha \cong A \cong B \cong 10 + \left(\frac{\langle N \rangle}{3.05} \right)^6, \quad (40)$$

$$P(0) = 0.5 \exp \left(-\frac{\langle N \rangle}{0.7} \right). \quad (41)$$

Table II shows results for broader jets with $R = 0.6$. Dependence of the parameters on $\langle N \rangle$ in this case are as follows:

$$\delta = 0.66 + \left(\frac{\langle N \rangle}{6.38} \right)^{5.85}, \quad (42)$$

$$\alpha_0 = -9.56 + 2.17 \langle N \rangle, \quad (43)$$

$$\alpha \cong A \cong B \cong 15.5 + \left(\frac{\langle N \rangle}{5.9} \right)^{17.5}, \quad (44)$$

Dependence of $P(0)$ on $\langle N \rangle$ remains the same as in Eq. (41).

The value of $\langle N \rangle$ increases by a factor of 1.85 for $R = 0.6$ in comparison to the case of $R = 0.4$ as seen from

TABLE I. Dependence on p_T^{jet} for $R = 0.4$ and $0 < |y| < 1.9$.

p_T^{jet} [GeV]	$\langle N \rangle$	$Var(N)$	A	B	α	δ	α_0	$P(0)$
4 – 6	3.303	1.730	13.3	10.3	14.596	1.176	0.286	0.00430246
6 – 10	4.131	2.585	15.7	13.0	16.287	1.387	2.096	0.00155689
10 – 15	5.170	3.946	32.7	27.9	29.374	2.220	4.367	0.000320975
15 – 24	6.254	5.612	127.0	125.0	126.666	3.938	6.055	0.0000309069
24 – 40	7.644	7.584	196.0	180.0	179.212	7.0	7.63	0.0000160399

TABLE II. Dependence on p_T^{jet} for $R = 0.6$ and $0 < |y| < 1.9$.

p_T^{jet} [GeV]	$\langle N \rangle$	$Var(N)$	A	B	α	δ	α_0	$P(0)$
4 – 6	4.398	2.319	17.4	13.2	20.216	0.961089	0.0	0.000767709
6 – 10	5.717	3.878	15.7	11.0	16.709	0.914	2.528	0.000272948
10 – 15	7.374	6.878	63.2	58.0	58.875	3.167	7.209	0.0000273138
15 – 24	8.526	8.420	577.7	580.0	579.390	6.168	68.509	0.00000141011
24 – 40	9.790	10.775	3.3	5.9	226.418	-0.00412	-218.809	0.000123035

TABLE III. Dependence on rapidity interval $|y|$ for $R = 0.4$ and $10 < p_T^{jet} < 15$ GeV.

$ y $	$\langle N \rangle$	$Var(N)$	A	B	α	δ	α_0	$P(0)$
0 – 0.5	5.246	3.086	24.4	27.0	27.861	2.227	4.507	0.000330263
0.5 – 1	5.178	3.949	47.3	44.0	46.500	2.631	4.483	0.000185273
1 – 1.5	5.158	3.852	15.7	17.0	18.476	1.677	4.012	0.00052248
1.5 – 1.9	5.061	3.854	30.7	31.0	32.632	2.370	4.310	0.000320779

the comparison of Tables I and II. Other dependencies on $\langle N \rangle$ are similar to those from the above equations. However, in the interval of $24 \text{ GeV} < p_T^{\text{jet}} < 40 \text{ GeV}$, we have $\delta < 0$ and hence, this p_T^{jet} interval was omitted in determining the parameter dependence on $\langle N \rangle$.

With regards to the relation between $\text{Var}(N)$ and $\langle N \rangle$, it is observed that for $R = 0.4$, we have dispersion $\sigma = \sqrt{\text{Var}(N)} = 0.33\langle N \rangle + 0.23$ and for $R = 0.6$ we have $\sqrt{\text{Var}(N)} = 0.33\langle N \rangle + 0.10$ ¹.

Note that mean multiplicities $\langle N \rangle$ within the various rapidity intervals do not depend significantly on the rapidity interval $|y|$, as shown in Table III, and are similar to $\langle N \rangle$ for the maximal interval $0 < |y| < 1.9$. Similarly, the other parameters do not differ significantly from the corresponding parameters in the maximum rapidity range (no systematic changes with the width of the rapidity range).

V. CONCLUSIONS

Recurrent relation $g(N) = (N + 1)P(N + 1)/P(N)$ leads to multiplicity distributions of the form

$$P(N) = \frac{P(0)}{N!} \prod_{i=0}^{N-1} g(i). \quad (45)$$

For $g(N)$ given by Eq. (20) with $\alpha_0 = 0$, we have PD for $\delta = 0$, a sub-Poissonian distribution for $\delta > 0$ also known as the Conway-Maxwell-Poisson distribution (COM-PD) [26–30] and a super-Poissonian distribution for $\delta < 0$.

It turns out, however, that the multiplicity distributions in jets prefer the recurrent relation with $\alpha_0 \neq 0$ leading to multiplicity distributions of the form given by Eq. (21). For small $\langle N \rangle$ we observe sub-Poissonian distributions with modified combinatorics oscillating as

$$\langle N \rangle C_j \propto (-1)^j \alpha^{j+1}. \quad (46)$$

Parameters of multiplicity distributions (α , α_0 and δ) depend on $\langle N \rangle$. For large $\langle N \rangle$, distributions are super-Poissonian when $-1 < \delta < 0$ ².

A sub-Poissonian distribution with $\text{Var}(N) < \langle N \rangle$ has not been very popular in the majority of discussions about multiplicity distributions in high-energy physics so far (mainly due the fact that this phenomenon is only observed when $\langle N \rangle$ is not too large). However, it is quite

an important distribution [17, 34]. The existence of a sub-Poissonian distribution implies at least one of the following scenarios: (1) the underlying elementary processes are not totally random (partially deterministic); (2) the classical Markov processes describing them require further generalizations. Either conclusion forces us to modify the successful stochastic approach. In our case, we show that the sub-Poissonian multiplicity distributions describing the experimental data can be naturally interpreted as stochastic Markov processes in which the birth and death rates are both multiplicity-dependent.

Acknowledgements

This research was supported in part by the National Science Centre, Poland (NCN) Grant 2020/39/O/ST2/00277 (MR) and by grants UMO-2016/22/M/ST2/00176 and DIR/WK/2016/2018/17-1 (GW). H.W. Ang would like to thank the NUS Research Scholarship for supporting this study. In preparation of this work we used the resources of the Center for Computation and Computational Modeling of the Faculty of Exact and Natural Sciences of the Jan Kochanowski University in Kielce.

Appendix A: Relationship of combinatorics with factorial moments and cumulants

Usually information contained in $P(N)$ is obtained by examining their corresponding factorial moments, F_q , and cumulant factorial moments, K_q , (or their ratios) (cf., [1, 2]),

$$K_q = F_q - \sum_{i=1}^{q-1} \binom{q-1}{i-1} K_{q-i} F_i, \quad (A1)$$

where

$$F_q = \sum_{N=q}^{\infty} N(N-1)(N-2)\dots(N-q+1)P(N), \quad (A2)$$

are the factorial moments. As shown in [9, 11] the K_q can be expressed as an infinite series of the C_j ,

$$K_q = \sum_{j=q}^{\infty} \frac{(j-1)!}{(j-q)!} \langle N \rangle C_{j-1}, \quad (A3)$$

and, conversely, the C_j can be expressed in terms of the K_q [1, 2],

$$C_j = \frac{1}{\langle N \rangle} \frac{1}{(j-1)!} \sum_{p=0}^{\infty} \frac{(-1)^p}{p!} K_{p+j}. \quad (A4)$$

Note that C_j depends only on multiplicities smaller than their rank [14, 15] while moments K_q require the knowledge of all $P(N)$ and therefore are very sensitive to possible limitations of the available phase space [1, 2]. On the other hand, calculations of combinatorics require the knowledge of $P(0)$ which may not always be available. Both C_j and K_q exhibit the property of additivity.

¹ It is worth recalling at this point that this linear relationship, $\sqrt{\text{Var}(N)} = a\langle N \rangle + b$, known as Wróblewski's law [31], is satisfied for a wide range of multiparticle production processes like pp collisions (here $a = -b = 0.585$), both π^+p and π^-p collisions (with $a = 0.44$ for π^\pm and $b = -0.22$ for π^+ and $b = -0.9$ for π^-) [32] and for e^+e^- (where $a = 0.25$ and $b = 0.7$) [33].

² For $\delta = -1$ we have well known NBD, for $\alpha_0 > \alpha > 0$ (where parameter $k = \alpha_0/\alpha + 1$, if additionally $\alpha_0 = 0$ we would have geometrical distribution, the most wide one) or BD for $\alpha_0 > 0$ and $\alpha < 0$ (where parameter $K = -\alpha_0/\alpha - 1$).

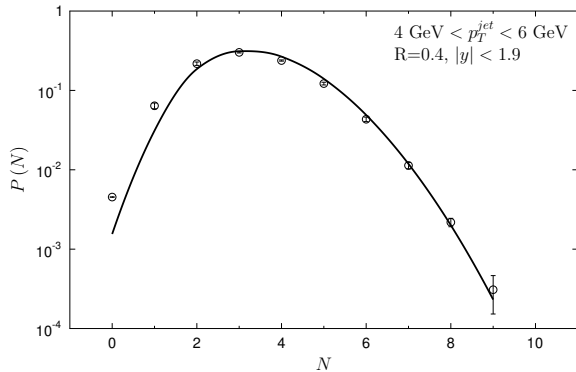


FIG. 7. Points: $P(N)$ from ATLAS data for jets with $4 \text{ GeV} < p_T^{jet} < 6 \text{ GeV}$ and radius parameter $R = 0.4$, over the full measured rapidity range $|y| < 1.9$. The curve fitting these data comes from generating function given by Eq. (B2).

Appendix B: Multiplicities from two Binomial Distributions

If we have two sources producing N_1 and N_2 particles respectively and each distributed according to BD defined by parameters (K_1, p_1) and (K_2, p_2) , then the distribution of $N = N_1 + N_2$ particles,

$$P(N) = \sum_{i=0}^{\min(N, K_1, K_2)} P_1(i)P_2(N-i), \quad (\text{B1})$$

is described by a generating function comprising the product of generating functions for both sources, i.e. by

$$G(z) = (1 - p_1 + p_1 z)^{K_1} \cdot (1 - p_2 + p_2 z)^{K_2} \quad (\text{B2})$$

In this case, the first two moments of the distribution $P(N)$ are given by

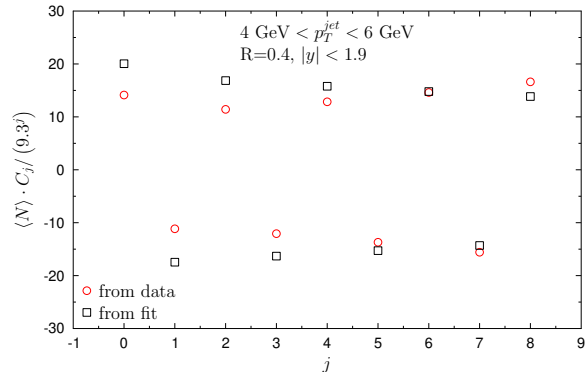


FIG. 8. Comparison of C_j for multiplicity distributions from Fig. 7. Red circles: C_j from data on $P(N)$, black squares: C_j from Eq. (B4) obtained from theoretical $P(N)$ defined by the generating function given by Eq. (B2).

$$\begin{aligned} \langle N \rangle &= \left. \frac{dG(z)}{dz} \right|_{z=1} = K_1 p_1 + K_2 p_2, \quad (\text{B3}) \\ \text{Var}(N) &= \left. \frac{d^2 G(z)}{dz^2} \right|_{z=1} + \langle N \rangle - \langle N \rangle^2 = \\ &= K_1 p_1 (1 - p_1) + K_2 p_2 (1 - p_2). \quad (\text{B4}) \end{aligned}$$

Denoting the modified combinatorial of the first and second BD component as $C(1)_j$ and $C(2)_j$ respectively, the overall modified combinatorial $\langle N \rangle C_j$ can be written as

$$\begin{aligned} \langle N \rangle C_j &= \langle N_1 \rangle C(1)_j + \langle N_2 \rangle C(2)_j = \quad (\text{B5}) \\ &= (-1)^j \left\{ K_1 \left[\frac{p_1}{(1-p_1)} \right]^{j+1} + K_2 \left[\frac{p_2}{(1-p_2)} \right]^{j+1} \right\}. \end{aligned}$$

The value of one of the p parameters must be carefully chosen to reflect the observed increase in the amplitude of C_j . Choosing (indicative) $K_1 = 2$, $p_1 = 0.9$ and $K_2 = 10$, $p_2 = 0.17$ we have $P(N)$ and C_j as shown in Figs. 7 and 8. For this set of parameters used to fit data, we have $\langle N \rangle = 3.5$ and $\text{Var}(N) = 1.6$.

While it is possible to reasonably describe either $P(N)$ or C_j with a suitable choice of parameters, it is not yet possible to describe both simultaneously. Figs. 7 and 8 show the extent of deviation from data of such an approach.

It turns out that while by suitable choice of parameters, we can describe (more or less reasonably) separately $P(N)$ or C_j , but not simultaneously both observables. Figs. 7 and 8 demonstrate to what extent is it possible to get closer to this goal in such an approach.

-
- [1] W. Kittel and E. A. De Wolf, *Soft Multihadron Dynamics*, World Scientific, Singapore (2005).
[2] R. Botet and M. Płoszajczak, *Universal fluctuations, The phenomenology of hadronic matter*, World Scientific, Singapore (2002).
[3] T.F Hoang, B. Cork, Z. Phys. C **36**, 323 (1987).

- [4] S.V. Chekanov, V.I. Kuvshinov, J. Phys. G **22**, 601 (1996).
[5] I. Zborovsky, *Multiplicity distributions in proton-(anti)proton and electron-positron collisions with parton recombination* arXiv:1106.4697 [hep-ph] (2011).
[6] B.E.A.Saleh and M.K. Teich, Proc. IEEE **70**, 229 (1982).

- [7] G. Wilk, Z. Włodarczyk, *J. Phys. G* **44**, 015002 (2017).
- [8] G. Wilk and Z. Włodarczyk, *Int. J. Mod. Phys. A* **33**, 1830008 (2018).
- [9] M. Rybczyński, G. Wilk, Z. Włodarczyk, *Phys. Rev. D* **99**, 094045 (2019).
- [10] H.W. Ang, M. Ghaffar, A.H.Chan, M. Rybczyński, Z. Włodarczyk, G. Wilk, *Mod. Phys. Lett. A* **34**, 1950324 (2019).
- [11] H.W. Ang, A.H. Chan, M. Ghaffar, M. Rybczyński, G. Wilk, Z. Włodarczyk, *Eur. Phys. J. A* **56**, 117 (2020).
- [12] G. Wilk, Z. Włodarczyk, *Int. J. Mod. Phys. A* **36**, 2150072 (2021).
- [13] I. Zborovsky, *Eur. Phys. J. C* **78**, 816 (2018).
- [14] S.K. Kauffmann and M. Gyulassy, *J. Phys. A* **11**, 1715 (1978).
- [15] M. Gyulassy, S.K. Kauffman, *Phys. Rev. Lett.* **40**, 298 (1978).
- [16] R. Vasuvedan, P. R. Vitall, K. V. Parthasarathy, *J. Phys. A* **17**, 989 (1984).
- [17] P. Carruthers, C.C. Shih, *Int. J. Mod. Phys. A* **2**, 1447 (1987).
- [18] A.B. Balantekin and J.E. Seger, *Phys. Lett. B* **266**, 231 (1991).
- [19] I. Szapudi and A. S. Szalay, *Astrophys. J.* **408**, 43 (1993).
- [20] S.J. Lee and A.Z. Mekjian, *Nucl. Phys. A* **730**, 514 (2004).
- [21] A.Z. Mekjian, T. Csörgö and S. Hegyi, *Nucl. Phys. A* **784**, 515 (2007).
- [22] G. Aad et al. (ATLAS Collaboration), *Phys. Rev. D* **84**, 054001 (2011).
- [23] Durham HepData Project: <https://www.hepdata.net/record/57743?>
- [24] G. Wilk, Z. Włodarczyk, *Phys. Lett. B* **727**, 163 (2013).
- [25] N. G. Watson, *A treatise on the theory of Bessel functions*, 2nd edn (Cambridge University Press, 1944). pp. 500-501.
- [26] R. W. Conway, W. L. Maxwell, *J. Industrial Engin.* **12**, 132 (1962).
- [27] G. Shmueli, T. P. Minka, J. B. Kadane, S. Borle, P. Boatwright, *J. Royal Stat. Soc. C (Applied Statistics)* **54**, 127 (2005).
- [28] S. Chakraborty, T. Imoto, *J. Stat. Distr. & Appl.* **3**, 1 (2016); DOI: 10.1186/s40488-016-0044-1.
- [29] S. B. Chatla, G. Shmueli, *Comp. Stat. & Data Ana.* **121**, 71 (2018).
- [30] B. Li, H. Zhang, J. He, *Comm. Stat. -Theory & Methods* **49**, 1311 (2020); DOI:10.1080/03610926.2018.1563164.
- [31] A. K. Wróblewski, *Acta Phys. Pol. B* **4** (1973) 857.
- [32] L. Van Hove, *Phys. Lett. B* **43** (1973) 65.
- [33] R. Szwed, G. Wrochna, A.K. Wróblewski, *Mod. Phys. Lett. A* **5** (1990) 1851.
- [34] C. C. Shih, *Phys Rev D* **34** (1986) 272.